JOURNAL OF AIRCRAFT
Vol. 46, No. 1, January–February 2009

Impact of the Reduced Vertical Separation Minimum on the Domestic United States

Andrew Malwitz,* Sathya Balasubramanian,† and Gregg Fleming‡
John A. Volpe National Transportation Systems Center, Cambridge, Massachusetts 02142
and
Timothy Yoder§ and Ian Waitz¶
Massachusetts Institute of Technology, Cambridge, Massachusetts 02139

DOI: 10.2514/1.36776

Aviation regulatory bodies have enacted the reduced vertical separation minimum standard over most of the globe. The reduced vertical separation minimum is a technique that reduces the minimum vertical separation distance between aircraft from 2000 to 1000 ft, for cruise altitudes between 29,000 and 41,000 ft. It was first introduced over the North Atlantic in March 1997, and, more recently, over the domestic U.S. in January, 2005. Previous studies by EUROCONTROL and the Federal Aviation Administration have found that, by allowing for more efficient flight trajectories, the implementation of reduced vertical separation minimum can reduce fuel burn and related emissions by 1.5%–3%. However, the modeling techniques used in these prior studies did not directly include weather or the influence on changes in engine-specific fuel consumption with throttle setting, Mach number, or altitude. Because of the influence that these factors may have on accurately predicting changes in fuel burn with small changes in aircraft operations, we sought to assess the influence of these assumptions, to develop improved modeling methods, and to use these improved methods to make a new estimate of the impacts of the reduced vertical separation minimum. This document estimates the impact of reduced vertical separation minimum within the continental U.S. for a sample of 100,000 radar-based flight trajectories. We incorporated meteorological conditions resolved along the individual flight trajectories. Computer flight data recorder archives from 2800 flights were statistically analyzed to develop an improved model for estimating changes in aircraft fuel burn with changes in Mach number, throttle setting, and ambient conditions. Using these methods, we estimate that fuel burn and nitrogen oxide production per distance traveled decreased by about 2% and 3%, respectively, with the implementation of reduced vertical separation minimum over the continental U.S. Although our estimate for the benefits of reduced vertical separation minimum is similar to previous studies, we also show that the use of detailed meteorological conditions, and the advancements in aircraft fuel burn estimation described in this paper, are important for analyzing small changes in efficiency related to the implementation of reduced vertical separation minimum. In particular, if these advancements were not incorporated, the estimated benefits of reduced vertical separation minimum for this sample of 100,000 radar-based flight trajectories would be approximately 0%.

Nomenclature

C_D = coefficient of drag
C_L = coefficient of lift
D = total drag
g = acceleration due to gravity
M = Mach number
m = mass of aircraft
m_f = mass of the fuel
m_p = mass of the payload
N_g = engine shaft speed
S = wing reference area
s = time
T = thrust
V_{TAS} = true air speed
δ = ratio of at-altitude to sea-level pressure
$\Delta\eta$ = change in fuel efficiency
ΔX = distance traveled
η = fuel efficiency
θ = ratio of at-altitude to sea-level temperature
ρ = air density
τ = ratio of at-altitude to sea-level thrust

Received 24 January 2008; revision received 15 August 2008; accepted for publication 18 August 2008.

*Environmental Engineer, Volpe National Systems Center, 55 Broadway, Cambridge, MA 02142.

†Senior Software Engineer, Computer Science Corporation, 55 Broadway, Cambridge, MA 02142.

‡Division Chief, Volpe National Systems Center, 55 Broadway, Cambridge, MA 02142.

§Graduate Student, Department of Aeronautics and Astronautics, 77 Massachusetts Avenue, Cambridge, MA 02139.

¶Jerome C. Hunsaker Professor and Head, Department of Aeronautics and Astronautics, 33-207, 77 Massachusetts Avenue, Cambridge, MA 02139. Fellow AIAA.

I. Introduction

COMMERCIAL aircraft are responsible for approximately 13% of transportation-related fossil fuel consumption and approximately 2% of anthropogenic carbon dioxide emissions [1]. Additionally, most projections estimate that air travel will grow by 2 to 5% per year for the next 10 to 20 years [1]. Therefore, there is concern that the environmental impact of aviation, including the production of carbon dioxide and other greenhouse gases, will increase in the coming years. In addition, as air travel grows, the air transportation system is expected to become increasingly capacity constrained at some airports and along some flight corridors. The reduced vertical separation minimum (RVSM) standard was introduced to address the following areas of concern: airborne capacity, fuel consumption, and related emissions.

Beginning over the North Atlantic in March of 1997, and recently over the domestic U.S. in January of 2005, worldwide aviation regulatory bodies enacted the RVSM standard [2] as shown in Fig. 1. Before the new standard, the minimum separation for altitude between 29,000 and 41,000 ft was 2,000 ft. The new

RSVM standard reduced the minimum separation of aircraft between cruise altitudes to 1000 ft, creating six new cruising altitudes. With more cruise altitudes available, airspace capacity is increased. Additionally, aircraft may be flown at more fuel-efficient cruising altitudes.

Two previous studies estimated the fuel burn and emissions benefits of RVSM. The first study, conducted by EUROCONTROL [3], analyzed the impact of RVSM implementation in European airspace in January of 2002. The EUROCONTROL study found a benefit of 1.6 to 2.3% reduction in fuel burn, and 0.7 to 1.0% reduction in emissions of nitrogen oxides (NO_x) as a result of implementing RVSM. The second study, conducted by the Federal Aviation Administration (FAA) [4], analyzed the impact of RVSM implementation in U.S. airspace in January 2005 for 12 origin–destination pairs. The FAA study found that each flight in RVSM airspace saved approximately 3 lb (1.36 kg) of fuel per minute at cruise altitude, which is equivalent to an approximately 2.5% reduction in fuel burn and CO_2. However, the modeling techniques used in these prior studies did not directly include weather or the influence on engine-specific fuel consumption of changes with throttle setting, Mach number, or altitude. Because of the influence that these factors may have on accurately predicting changes in fuel burn with small changes in aircraft operations, this study sought to assess the influence of these assumptions, to develop improved modeling methods, and to use these improved methods to make a new estimate of the impacts of RVSM.

The study reported here investigated the impact of RVSM when it was enacted over the domestic U.S. in 2005 for a sample of 100,000 radar-based flight trajectories. We incorporated meteorological conditions resolved along the individual flight trajectories. Further, computer flight data recorder (CFDR) archives from 2800 flights were statistically analyzed to develop an improved model for estimating changes in aircraft fuel burn with changes in Mach number, throttle setting, and ambient conditions. The study was conducted jointly by the U.S. Department of Transportation's Volpe Center (Volpe) and the Massachusetts Institute of Technology (MIT), under the Partnership for Air Transportation Noise and Emission Reduction (PARTNER), for the FAA's Office of Environment and Energy (FAA/AEE).

II. Study Methodology

This assessment of the impact of the domestic U.S. implementation of RVSM on fuel burn and emissions required a source of schedule and flight trajectory data for a time frame that included both pre-RVSM and post-RVSM conditions in addition to an aircraft performance model capable of estimating small changes in performance with changing flight conditions and routing. For schedule and flight trajectory data, we used the Enhanced Traffic Management System (ETMS) [5]. ETMS is a tool used by the FAA for air traffic planning purposes. It contains both reported flight-plan data and position data obtained directly from radar sources. Thus, if a flight provides flight-plan information, and/or enters radar-controlled airspace, ETMS will have information on the flight schedule (such as departure/arrival time and airport), as well as position data (how the flight is flown in three-dimensional space). ETMS encompasses the North American airspace as well as portions of Western Europe.

The pre-RVSM period of study included domestic U.S. flights during four weeks before the January 2005 implementation of RVSM, and the post-RVSM period included domestic U.S. flights during four weeks after the implementation of RVSM. The weeks chosen for analysis were the same weeks used in the 2005 FAA study [4] and are summarized in Table 1. The weeks were chosen to avoid irregular holiday traffic in an effort to provide a more consistent comparison. In addition, the study was limited to flights that were represented in both scenarios. Thus, the pre- and post-RVSM scenarios had the same number of flights for distinct origin–destination pairs. We also limited the study to matched aircraft types so that there were no differences in the fleet between the pre- and post-RVSM analysis cases. In all, this study observed 100,000 radar-based trajectories from ETMS to investigate the impact of RVSM.

We used EUROCONTROL's Base of Aircraft Data Revision 3.6 (BADA) [6] to model en route aircraft performance. BADA was also used in the two prior studies [3,4] that estimated the impact of RVSM. EUROCONTROL developed BADA to provide trajectory simulation and prediction algorithms for air traffic management (ATM) purposes. It has been shown that, on a fleet-wide level, BADA can estimate fuel burn inventories to within 5% of airline-reported fuel burn values [7]. However, for specific flight conditions, BADA methods may produce fuel burn estimates with more than 20% error relative to reported values [7]. Because the previous studies indicate that the impact of RVSM can be less than the uncertainties of the BADA method, we sought to address some of the uncertainties in the BADA method for this study.

A previous study conducted by the FAA quantitatively ranked the largest errors in BADA fuel burn estimates (when using no wind data and standard atmospheric conditions) as the following uncertainties

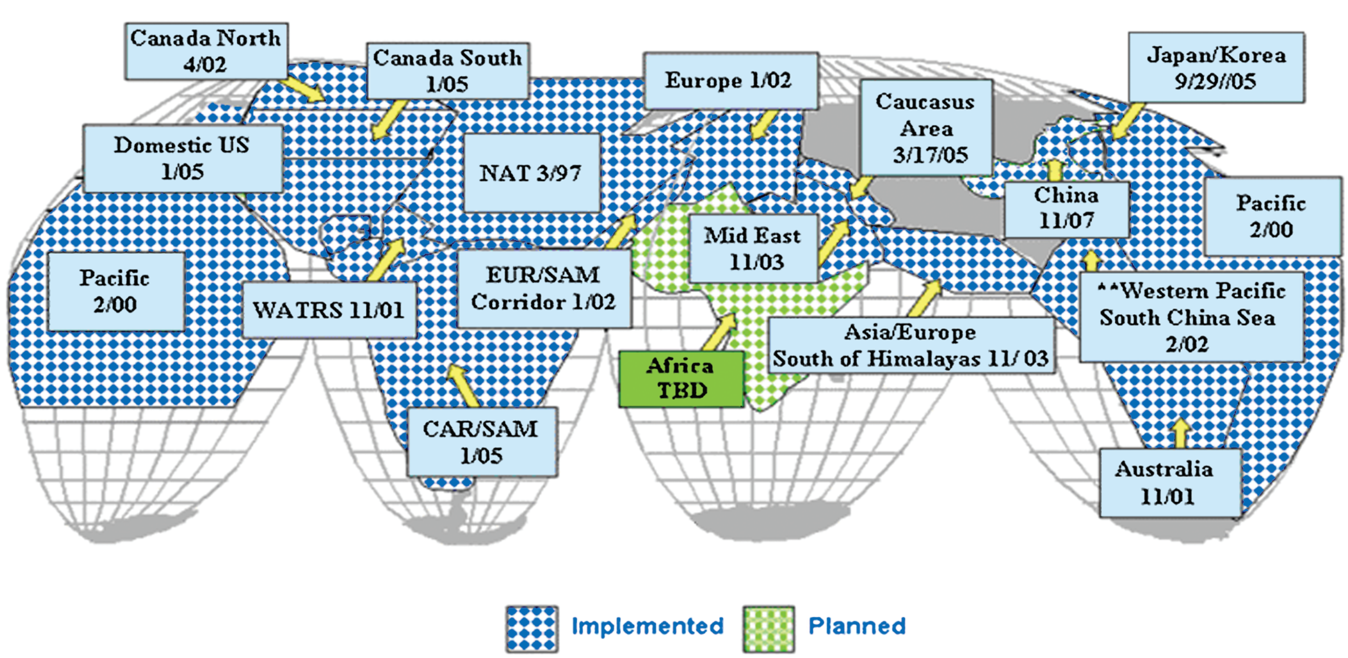

Fig. 1 Dates of RVSM worldwide [2].

Table 1 Pre-RVSM and post-RVSM dates

	Dates	Days
Pre-RVSM	11/14/2004-11/20/2004	7
	12/05/2004-12/18/2004	14
	1/9/2005-1/15/2005	7
	Pre-RVSM total	28
Post-RVSM	2/13/2005-3/12/2005	28
	Post-RVSM total	28
	Grand total	56

(in order of importance): aircraft drag coefficients, engine performance coefficients, variation in winds aloft, takeoff weight, and temperature at cruise altitudes, respectively [7]. Our study addressed three of these concerns: winds aloft, temperature at cruise, and engine performance coefficients. Winds aloft and temperature at cruise were addressed by including detailed meteorological data. To help minimize the uncertainty due to aircraft weights, we chose weeks in which load factor would not greatly vary (for instance, due to holiday travel). Uncertainty due to aircraft weights is discussed further in Sec. VII.

To estimate the impact of RVSM, our primary concern for alternative aircraft performance calculations was to include a functional dependence due to variations in cruise altitude. The BADA aircraft drag estimate already includes these dependencies; however, the engine performance estimate does not. The uncertainty in the BADA aircraft drag estimate was not addressed in this study.

III. Inclusion of Meteorological Data

BADA as well as many other aircraft performance models compute fuel burn as a function of aircraft thrust. For most of the flight regimes observed in this study (i.e., steady, level, cruise flight conditions undergoing no climb or descent and no acceleration), thrust is assumed to equal drag. For flight conditions where this is not the case, such as takeoff and arrival procedures or acceleration and climb operations during cruise, thrust power minus drag power equals the change in kinetic or potential energy of the vehicle as a function of time. Thus, a power balance is used to compute thrust as a function of drag, velocity, and changes in aircraft kinetic and potential energy. For all drag computations, BADA uses the following equation:

$$D = (C_D \rho V_{\mathrm{TAS}}{}^2 S)/2 \tag{1}$$

The drag coefficient, C_D, is then determined using aircraft-type-specific BADA coefficients C_{d0} and C_{d2}. Additionally, a non-BADA correction for transonic drag rise, ΔC_{DC}, described by Yoder [8], is included due to the use of speeds reported from radar and not the default or nominal speeds provided from BADA. This correction enables a better representation of the functional dependence of the drag coefficient on flight Mach number

$$C_D = C_{d0} + C_{d2}(C_L)^2 + \Delta C_{dC} \tag{2}$$

$$C_L = \frac{2mg}{\rho V_{\mathrm{TAS}}{}^2 S} \tag{3}$$

True air speed is defined as the speed in which an aircraft moves through its local air medium. Because we use radar data for flight trajectories, we have a radar-inferred measure of ground speed. If wind data are not used, ground speed is typically approximated as being equal to true air speed. If a flight experiences a head wind, the true air speed appears less than it actually is, and thus drag, thrust, and fuel burn are underestimated; conversely, if a flight experiences a tail wind, air speed appears greater than it actually is, and thus drag, thrust, and fuel burn are overestimated. True air speed can be better approximated if wind data are used. We performed vector addition and subtraction between the aircraft ground speed and wind speed vectors to achieve a true speed approximation.

Air density is related to the air pressure and temperature (i.e., by the ideal gas law). Typically, in flight trajectory computations for aircraft flight levels below 11,000 m (about 36,000 ft), temperature is assumed to be 288.15 K at sea level, lapsing at a rate of 0.0065 K for every meter of elevation; pressure is assumed to be 101,325 Pa at sea level, lapsing as a ratio of sea level to ambient temperature. Above 11,000 m (the region of the atmosphere known as the tropopause), temperature is held constant, and a separate equation is used to compute pressure. The drag estimate can be further improved if more accurate estimates of temperature and pressure are used.

The meteorological information we used was from the Goddard Earth Observing System (GEOS). GEOS is a division of the Goddard Earth Sciences Data and Information Services Center. The meteorological information has a spatial resolution of 1.25 deg by 1 deg, is updated every 6 hours, and includes temperature, wind speed and direction, at 36 distinct pressure levels ranging from 0.2 to 1000 hPa [9]. To approximate meteorological data for all aircraft positions, the data were interpolated between data points (time, latitude, longitude, and pressure levels).

IV. CFDR-Derived Fuel Burn Computation

To calculate fuel burn, BADA uses Eq. (4) during takeoff and landing procedures [any portion of the flight below 25,000 ft msl (mean sea level)], and Eq. (5) during cruise (any portion of the flight above 25,000 ft msl):

$$f = s^* \mathrm{SFC}_{\mathrm{BADA}}{}^* T \tag{4}$$

$$f = s^* \mathrm{SFC}_{\mathrm{BADA}}{}^* T^* C_{\mathrm{fcr}} \tag{5}$$

where f is the fuel burn during some portion of the flight, s is measured in minutes, C_{fcr} is a constant unique for each aircraft, and SFC is the specific fuel consumption. SFC is a measure of the rate at which an engine consumes fuel (in BADA, it is presented in terms of kilograms of fuel per minute per kiloNewton of thrust). The standard SFC equation for jet aircraft in BADA for the complete range of aircraft flight operation (takeoff, cruise, and descent) is

$$\mathrm{SFC}_{\mathrm{BADA}} = C_{f1}\left(1 + \frac{V_{\mathrm{TAS}}}{C_{f2}}\right) \tag{6}$$

where C_{f1} and C_{f2} and are constants unique for each aircraft. This SFC equation for BADA, along with all of the unique aircraft constants (C_{f1}, C_{f2}, and C_{fcr}), are the same for all conditions and segments of a complete aircraft operation (with the exception of the C_{fcr} constant for altitudes above 25,000 ft msl). Therefore, any variation of atmospheric conditions or throttle setting related to changes in cruise altitude (e.g., from RVSM) will not be reflected in the SFC estimate. The rate at which an engine consumes fuel for a given thrust and true air speed will remain constant. This is not an accurate representation of the behavior of gas turbine engines [10].

To account for the variability of engine performance with meteorological conditions and throttle setting, we derived a new equation for SFC that can also be used with the standard BADA method. To develop this new SFC equation, we acquired CFDR information for over 2800 flights, representing 12 different aircraft/engine combinations, and about 7% of the global fleet, or 5% of the U.S. fleet. A list of the aircraft/engine combinations and the number of flights of CFDR data for each is provided in Table 2.

SFC depends on ambient temperature and pressure, Mach number, and net thrust. For our RVSM analysis, ambient temperature and pressure were acquired directly from the weather data noted earlier and reflect changes in ambient conditions resultant from RVSM (varying cruise altitudes). The Mach number was acquired from flight trajectories, and net thrust was acquired from BADA estimates.

Using nondimensional parameters, (for example, see the textbook *Mechanics and Thermodynamics of Propulsion* [10]), we represented SFC using the following relationship:

Table 2 Available CFDR data

Aircraft type	Engine type	Number of flights
A319	CFM56-5B5-2	191
A320-214	CFM56-5B4-2	240
A321	CFM56-5B1-2	176
A330-202	PW4168	224
A330-243	RRTrent700	238
A330-223	PW4168A	264
A340-300	CFM56-5C4/P	188
A340-500	RRTrent500	262
B757-200	RB211-535C	178
B767-300	CF6-80C2	222
B777-300ER	GE90-115B1	365
ARJ85	LF507-1F	266

$$\frac{\mathrm{SFC}}{\sqrt{\theta}} = f\left(M, \frac{N_g}{\sqrt{\theta}}, Re\right) \tag{7}$$

The Reynolds number is not significant when compared with the effects of the Mach number or shaft speed, and the dependence of SFC on shaft speed can be modeled with an exponential function. Therefore, the relationship between shaft speed and thrust may be represented with the following function:

$$\frac{N_g}{\sqrt{\theta}} = \left(\frac{\tau}{\delta^{0.9}}\right)^{0.3} \tag{8}$$

Using Eqs. (7) and (8) we have a general relationship between SFC and the desired inputs (ambient temperature and pressure, Mach number, and thrust). The final function for SFC is provided here:

$$\frac{\mathrm{SFC}}{\sqrt{\theta}} = \alpha + \beta_1 M + \beta_2 e^{-\beta_3 (\frac{\tau}{\delta^{0.9}})^{0.3}} \tag{9}$$

where α, β_1, β_2, and β_3 are constants. (Note: this equation provides SFC in terms of kilograms of fuel per second per Newton). The equation does not include a constant factor to apply for portions of the flight above a certain altitude to represent a difference in fuel consumption between takeoff/landing procedures and cruise. We use this single equation, along with time elapsed and total thrust, to estimate fuel burn, and we do not have a modeling disconnect above and below a certain altitude (as in the instance of BADA, 25,000 ft msl). We performed a statistical analysis of CFDR data to determine coefficients for this relationship. The CFDR data contains, for every flight, segment-level data (Mach number, pressure, and the inferred net thrust taken from BADA) for the complete range of operation (departure gate to arrival gate). We performed the regression analysis to minimize the error in fuel burn between the model and the CFDR data. We did so for the full flight. Thus, the derived SFC equation will be applicable to the entire range of an aircraft operation. Table 3 presents the values for these four constants (and 95% confidence intervals for three of these constants; β_3 was not found through a least-squares analysis, but rather through an iterative process that minimized the residual's resultant from the other derived coefficients) for each aircraft present in the CFDR data.

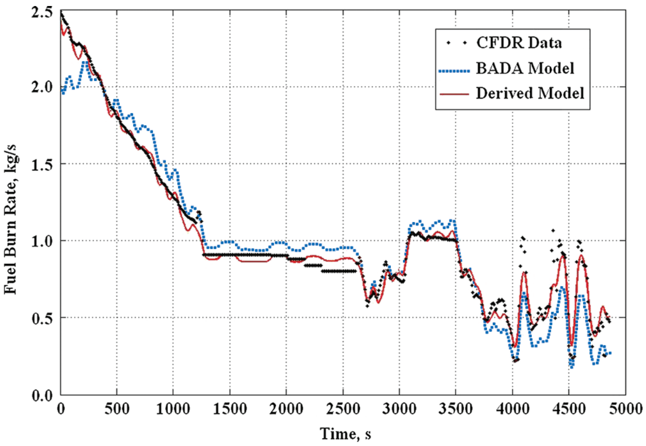

Fig. 2 Example comparison of fuel burn rate (B757-200).

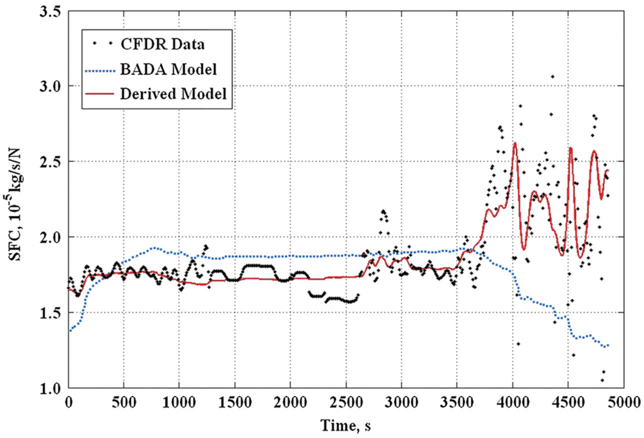

Fig. 3 Example comparison of SFC models (B757-200).

These fitted coefficients improve fuel burn modeling capability when compared with the original BADA methods for the specific aircraft types analyzed. Figures 2–5 provide a comparison of the results using the aircraft-specific SFC models derived here, the original BADA SFC model, and the estimates derived from the reported CFDR fuel flow data. Figures 2 and 3 show fuel burn and SFC, respectively, for the entirety (takeoff, cruise, and landing) of one example flight of a B757-200; Figs. 4 and 5 show fuel burn and SFC for the entirety (takeoff, cruise, and landing) of one example flight of an ARJ85. As shown in Figs. 2 and 4, the fuel burn estimate is comparable between the two modeling techniques (BADA and

Table 3 Derived aircraft-specific SFC coefficients

Aircraft type	α		β_1		β_2		β_3
	Value	95% CI	Value	95% CI	Value	95% CI	Value
A319	1.25E − 05	6.98E − 07	5.03E − 06	4.66E − 07	1.64E − 04	1.59E − 06	6.40E + 00
A320-214	1.13E − 05	2.24E − 07	7.84E − 06	3.32E − 07	1.46E − 04	3.14E − 05	5.70E + 00
A321	1.26E − 05	8.88E − 07	5.47E − 06	5.22E − 07	1.63E − 04	1.97E − 06	6.50E + 00
A330-202	1.11E − 05	2.18E − 07	7.46E − 06	2.78E − 07	6.79E − 05	6.11E − 05	5.00E + 00
A330-243	1.05E − 05	7.98E − 07	8.61E − 06	3.22E − 07	2.18E − 04	2.29E − 06	8.00E + 00
A330-223	1.05E − 05	3.56E − 07	8.38E − 06	9.43E − 08	1.47E − 04	1.08E − 06	7.50E + 00
A340-300	1.26E − 05	5.41E − 07	4.69E − 06	1.20E − 07	3.19E − 05	1.69E − 06	3.30E + 00
A340-500	9.52E − 06	2.66E − 07	8.38E − 06	7.25E − 08	1.95E − 04	8.33E − 07	6.60E + 00
B757-200	1.04E − 05	3.79E − 07	9.51E − 06	4.38E − 07	8.84E − 05	7.93E − 06	4.60E + 00
B767-300	1.45E − 05	4.08E − 07	2.87E − 06	4.27E − 08	1.38E − 04	1.13E − 06	8.90E + 00
B777-300ER	1.24E − 05	1.72E − 07	5.99E − 06	7.78E − 08	3.10E − 04	5.78E − 07	1.00E + 01
ARJ85	6.84E − 06	3.53E − 07	2.16E − 05	2.08E − 07	3.64E − 04	1.17E − 06	5.80E + 00

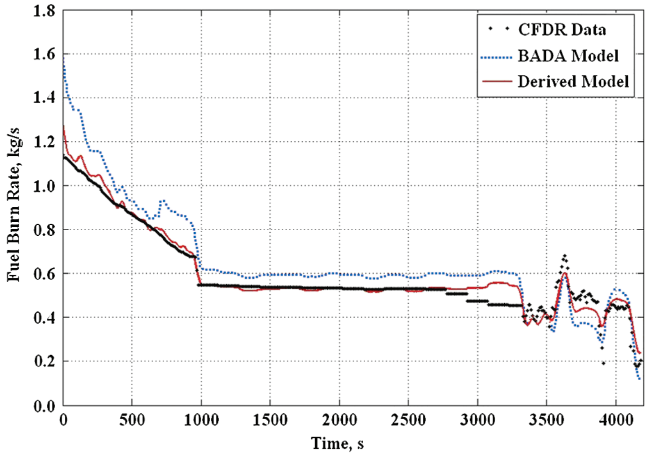

Fig. 4 Example Comparison of Fuel Burn Rate (ARJ85).

CFDR-derived) and reported CFDR values, and the overall fuel burn amount is dominated by aircraft procedures and operating conditions such as thrust, climb, and drag. For instance, in the B757-200 example (Fig. 2), both modeling techniques capture that the first 1200 s of the flight is a takeoff-to-climb procedure (maximum thrust and fuel flow initially, then slowly reducing as the aircraft continues to climb), as well as capturing the cruise procedure from 1200 to 3500 s (long portions of constant thrust and fuel burn rate). The CFDR-derived SFC estimate demonstrates relatively small improvements in the overall fuel flow estimate. However, Figs. 3 and 5 identify the ability of the CFDR-derived SFC estimate to capture the effects of ambient conditions and operational factors, and that these conditions and factors are significant in improving the fidelity of the SFC estimate. Both the BADA and CFDR-derived SFC estimates, again, presume that the BADA drag and thrust estimates are accurate.

Figure 6 shows a comparison of the fuel burn error (CFDR-reported fuel burn vs computed fuel burn) for each aircraft in the CFDR data set using the two modeling techniques: traditional BADA equations and BADA thrust and drag estimates used with the SFC equation derived from statistical analysis of the CFDR data. Using both the BADA and CFDR-derived SFC equation, we estimated fuel burn for each flight present in the CFDR data set and calculated an absolute error by comparing the estimated fuel burn values with values from CFDR. Next, we determined the mean absolute error for each specific aircraft type across all flights present in the CFDR data set.

As shown in Fig. 6, the error for each aircraft type is reduced when the CFDR-derived SFC model is implemented. The CFDR-derived SFC model led to a 41% average reduction in mean absolute error across all 12 aircraft types. The comparison was made using the trajectory, weight, and meteorological information available from the CFDR data. Remaining errors in the fuel burn estimates are very likely due to inaccuracies in the aircraft-specific drag coefficients in the BADA model. However, as noted earlier, the BADA drag model contains the correct functional dependence on atmospheric and flight conditions, thus this study focused on improving the SFC model to allow SFC to be dependent on atmospheric and flight conditions.

The 12 aircraft–engine combinations in the CFDR data set are only a subset of the aircraft in the fleet. Therefore, a more general modeling technique was developed for application to other jet aircraft represented in BADA. (Note: BADA does include a model for nonjet aircraft, e.g., piston engine and turboprop-powered aircraft. However, because the total fuel burn from nonjet aircraft in the U.S. fleet is less than 5% of the overall U.S. commercial aviation fuel burn, and because RVSM does not generally affect these aircraft, we only derived a general SFC equation for jet-powered aircraft.) It was decided that the BADA constants used to calculate SFC (C_{f1}, C_{f2}, and C_{fcr}) needed to be incorporated in the CFDR-derived SFC equation noted earlier. In Eq. (9), the α term most closely links to the BADA aircraft-specific constants, as α is not dependent on Mach number, pressure, or thrust ratio. Thus, we approximated a relationship between α and the BADA aircraft-specific constants in the following manner: average values for β_1, β_2 and β_3 were calculated across all 12 aircraft types in the CFDR data set; next, α was solved using an iterative process to determine the form of the equation and a least-squares regression to determine the value of the constants. The final formula for α is presented here:

$$\alpha = \frac{C_{fl1}}{60,000}\left(1 + \frac{1.9438(240)}{C_{fl2}}\right)C_{\text{fcr}} - 5.3(10)^{-6} \qquad (10)$$

Thus, BADA-derived coefficients may be used within our SFC equation to provide a general SFC approximation. (Note: the 60,000 in the denominator represents the unit conversions of minutes to seconds (60) and kilo-Newtons to Newtons (1000); the 1.9438 in the numerator represents the unit conversion of knots to meters per second). For the β_1, β_2, and β_3 terms, the average values from the CFDR-derived aircraft constants were used (the 90% confidence intervals are provided also):

$$\beta_1 = 7.70(10)^{-6} \pm 7.4347(10)^{-6} \qquad (11)$$

$$\beta_2 = 1.86(10)^{-4} \pm 1.49(10)^{-4} \qquad (12)$$

$$\beta_3 = 6.75 \pm 2.94 \qquad (13)$$

Figures 7–9 provide a comparison of three SFC computations to the SFC values estimated from CFDR data (using the BADA drag model as described earlier) for three aircraft. The three different methods for computing SFC shown are: a) the aircraft-specific, CFDR-derived SFC; b) the generalized CFDR-derived SFC model

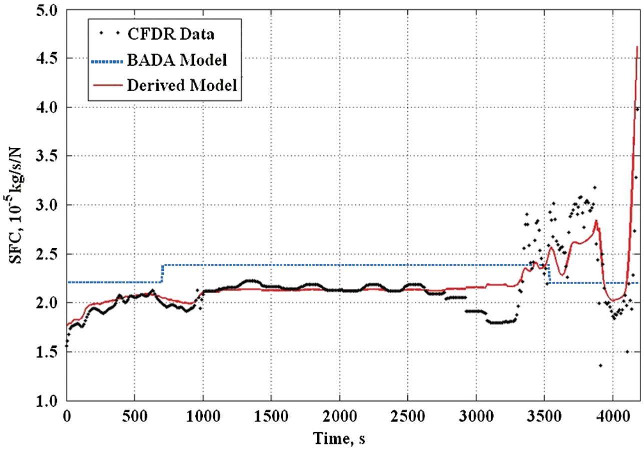

Fig. 5 Example Comparison of SFC Models (ARJ85).

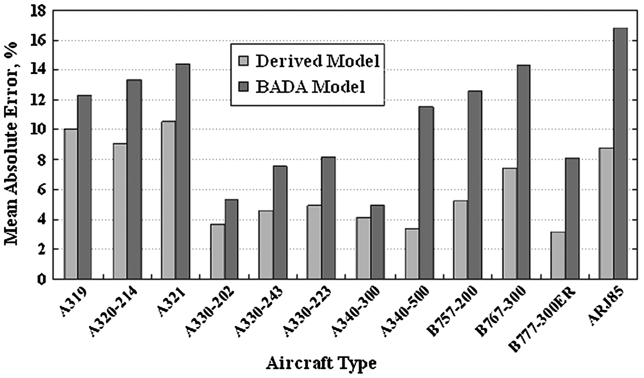

Fig. 6 SFC model error comparison.

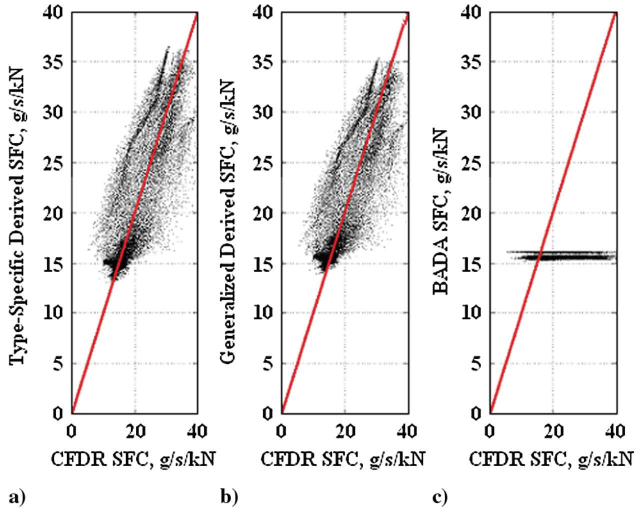

Fig. 7 SFC model comparison (A340-500).

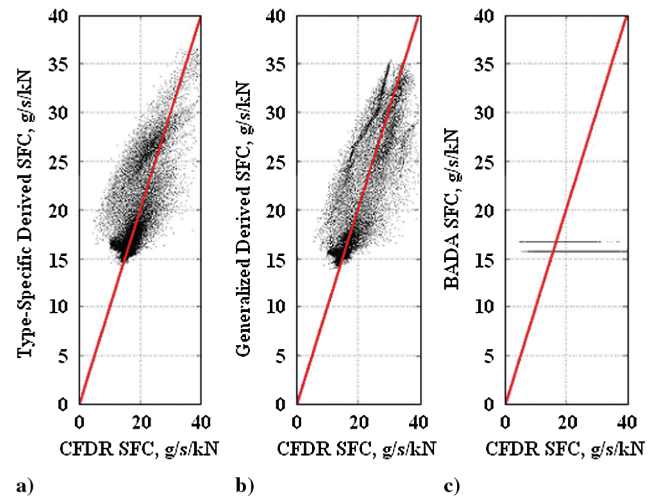

Fig. 9 SFC model comparison (A321-214).

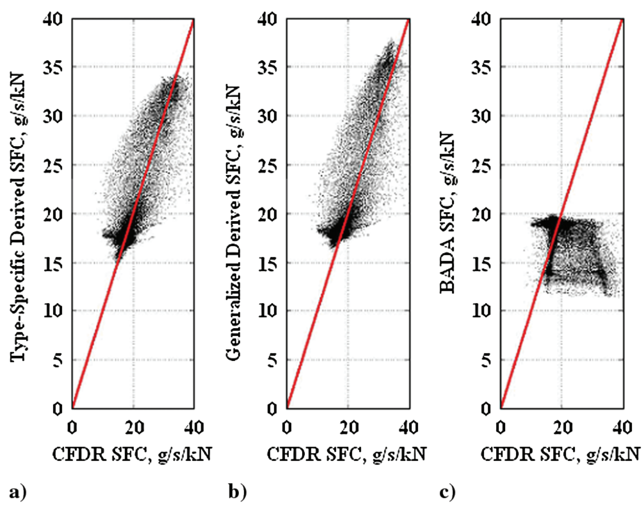

Fig. 8 SFC model comparison (B757-200).

that can be used with all BADA aircraft; and c) the original BADA SFC method.

As can be seen in these figures, the type-specific, CFDR-derived SFC method and the generalized CFDR-derived SFC method provide comparable results and improve significantly upon the SFC approximation from the original BADA methods. For instance, the original BADA methods generally hold constant as the SFC varies (as shown in Fig. 7 and 9). However, as the BADA SFC does vary with true air speed, some variation may occur (for instance, see Fig. 8). The process of generalizing the CFDR-derived SFC diminishes the accuracy somewhat as compared with the aircraft-specific, CFDR-derived model; however, the mean absolute error is still reduced by an average of 21% compared with the original BADA method. Of particular importance, the functional dependencies of important variables (such as throttle setting and meteorological conditions) are largely preserved in the generalized CFDR-derived SFC method, retaining the model's enhanced utility in evaluating operational alternatives.

V. RVSM Analysis

The general metric we used to assess fuel efficiency changes due to RVSM is fuel burn per distance traveled. We considered two distances, including the distance a flight traveled in relation to the ground (ground distance) and the distance a flight traveled in relation to local air space (air distance). The latter accounts for differences in routing due to winds and is more relevant for comparing pre-RVSM and post-RVSM aircraft performance because meteorological conditions were different between the two periods. To test the effect of our derived SFC equation and inclusion of meteorological conditions, we calculated fuel burn and emissions estimates for the pre- and post-RVSM periods using four techniques shown in Table 4.

Method 1 can be considered the typical implementation of BADA, with standard BADA equations using the Standard Atmosphere assumption. Methods 2, 3, and 4 make use of the GEOS weather data. Methods 3 and 4 also include the BADA drag prediction, but use the SFC equation derived from CFDR data. The aircraft-specific equations are used where available, and the general equation is used to model all remaining aircraft. Method 4 has the added improvement of measuring efficiency based on air distance traveled to better account for differences in winds aloft between the pre- and post-RVSM periods.

In addition to fuel burn calculations, we calculated nitrogen oxide (NOx) emissions for the entire range of the flight. This calculation was based on published engine emissions ratings from the International Civil Aviation Organization (ICAO) [11] and the Boeing Fuel Flow Method Version 2 (BFFM2) [12].

Our measure of efficiency was fuel burn per distance traveled in units of kilograms per nautical mile. We used the change in efficiency $\Delta\eta$ as a measure of the benefit associated with RVSM. The change in efficiency was calculated as

$$\Delta\eta = \frac{\eta_{\text{pre}} - \eta_{\text{post}}}{\eta_{\text{pre}}} \tag{14}$$

Table 4 Analysis technique assumptions

Method	Fuel burn model	Weather	Distance efficiency metric
1	BADA	Standard atmosphere	Ground
2	BADA	GEOS weather data	Ground
3	BADA drag, with derived SFC	GEOS weather data	Ground
4	BADA drag, with derived SFC	GEOS weather data	Air

Table 5 U.S. domestic RVSM analysis results (BADA Only)

Analysis method	Method 1: standard BADA with standard ISA, efficiency based on ground distance		Method 2: standard BADA with GEOS weather, efficiency based on ground distance	
Period	Pre	Post	Pre	Post
Number of flights	218,335			
Total distance, nm	123,734,247	123,841,509	123,540,856	123,551,562
Total fuel burn, kiloton	873.7	873.3	878.5	867.2
Total NOx, kiloton	11.43	11.37	11.61	11.34
$\Delta\eta$ fuel urn per distance, %	0.14		1.31	
$\Delta\eta$ NOx per distance, %	0.59		2.35	

Table 6 U.S. domestic RVSM analysis results (BADA only)

Analysis method	Method 3: BADA drag with GEOS weather and derived SFC, efficiency based on ground distance		Method 4: BADA drag with GEOS weather and derived SFC, efficiency based on air distance flown	
Period	Pre	Post	Pre	Post
Number of flights	218,335			
Total distance, nm	123,540,921	123,551,560	124,027,835	124,283,913
Total fuel burn, kiloton	843.0	829.8	843.0	829.8
Total NOx, kiloton	10.82	10.51	10.82	10.51
$\Delta\eta$ fuel burn per distance, %	1.61		1.81	
$\Delta\eta$ NOx per distance, %	2.94		3.14	

Thus, a positive $\Delta\eta$ indicates an increase or improvement in efficiency; that is, $\Delta\eta$ demonstrates the percentage in which fuel burn and emissions decreased as a result of RVSM.

We also estimated the variability of the results associated with the choice of time periods. Both of the original 28-day study periods were divided into two 14-day periods. The first two-week period of the pre-RVSM scenario (14 November 2004–20 November 2004 and 5 December 2004–11 December 2004) was compared with the first two-week period of the post-RVSM scenario (13 February 2005–26 February 2005); the second two-week period of the pre-RVSM scenario (12 December 2004–18 December 2004 and 9 January 2005–15 January 2005) was compared with the second two-week period of the post-RVSM scenario (27 February 2005–12 March 2005). The results of these two subanalyses differed somewhat from the aggregate results and were taken as an estimate of the potential variability due to the small (one month long) sample of flights considered. This variability was the basis for the estimated uncertainty in the aggregate results shown in Sec. VI. We note, however, that other sources of uncertainty exist and may be significant, including lack of knowledge of aircraft weight (discussed in Sec. VII) and uncertainties in the BADA aircraft drag computation (discussed previously in Sec. IV).

Finally, in an effort to substantiate the accuracy of the U.S. domestic comparison, we performed an additional comparison using ETMS data for flights in North Atlantic and European Union (EU) airspace. RVSM was implemented over the North Atlantic in 1997; therefore, the pre- and post-RVSM conditions in our study should have no discernible change in efficiency in this airspace. This was considered a control test of our methods, which is discussed further in the Results section.

VI. Results

The results of the U.S. domestic analysis are presented numerically in Tables 5 and 6, and graphically in Fig. 10 for each of the four analysis methods. Table 5 presents data calculated using the standard BADA method and two separate sources of meteorological data [standard ISA (international standard atmosphere) conditions and no winds aloft vs gridded meteorological conditions taken from GEOS]. Table 6 presents results calculated using the CFDR-derived SFC method and the GEOS meteorological conditions. The total fuel burn NOx and flight distance for all flights in the data analysis period and a system-wide efficiency were calculated.

As can be seen, the introduction of the CFDR-derived SFC equation further increases the estimated benefit of RVSM, albeit by a smaller amount (0.30% increase in fuel burn efficiency and 0.59% for NOx). Finally, when considering efficiency as measured by air distance flown, the fuel burn and NOx efficiencies increase by 0.2% compared with the third analysis method. Figure 10 presents all four computational methods together for comparison purposes. The error bands in this figure represent the variability of the efficiency metric. The first two weeks of the study were compared against the second two-week period of the study, and the variability between these two periods is represented in the error bands.

Overall, 70% of the difference in estimated efficiency benefit (both fuel and NOx) relative to the original BADA method can be attributed to including meteorological data, 18% to including a new SFC calculation, and 12% to measuring efficiency based on a metric of air distance traveled. Notably, without the inclusion of meteorological data and without the use of the improved SFC model, the estimated benefit of RVSM is approximately 0% as shown in Method 1 of Fig. 10.

The control comparison of the North Atlantic and EU region consisted only of a fuel burn comparison. As expected, it resulted in a nearly zero efficiency change when GEOS weather data, the derived SFC method, and the efficiency based on air distance were used. Wind patterns differed greatly over the North Atlantic between the pre- and post-RVSM scenarios (as shown in Fig. 11). Thus, the

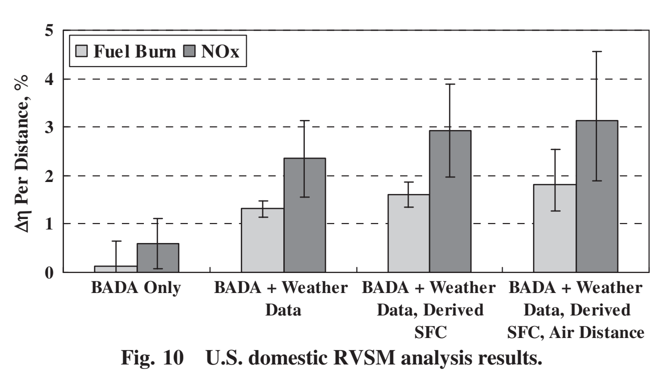

Fig. 10 U.S. domestic RVSM analysis results.

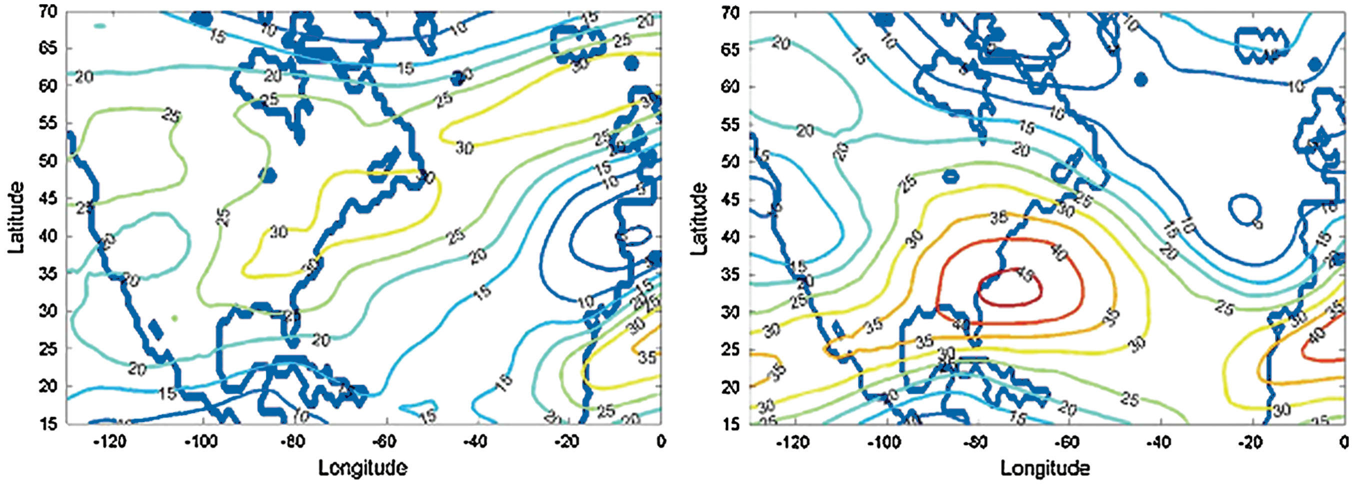

a) b)

Fig. 11 Comparison of average cruise altitude winds (presented as m/s) as derived from GEOS data set where a) represents pre-RVSM, and b) represents post-RVSM.

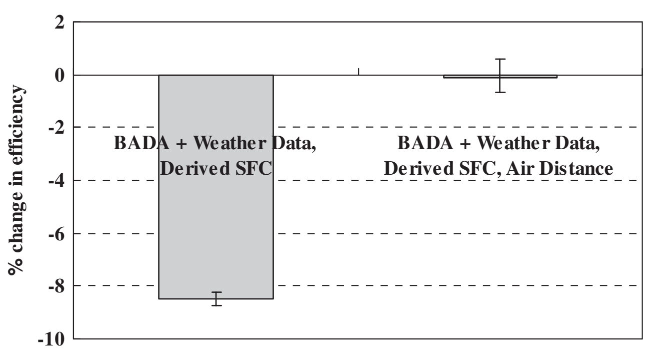

Fig. 12 North Atlantic and E.U. RVSM analysis results (control).

difference in wind velocity between the two study periods appears as a substantial negative change in efficiency if the ground distance is used, as shown in Fig. 12. Including the air distance efficiency resulted in an estimated efficiency change (pre- to post-RVSM) of only 0.012%, also shown in Fig. 12. This small difference in the control comparison provides support for the validity of the method, because the RVSM method was in place over the North Atlantic and EU during both periods of study.

VII. Effect of Aircraft Weight Estimates

As previously mentioned, one of the largest uncontrolled areas of uncertainty in this study is the use of standardized aircraft weight estimates that are a function of stage length, but that do not reflect potential differences in aircraft loading between the pre- and post-RVSM periods. If detailed information on aircraft weight or load factors were available, a more appropriate basis for comparison would be an efficiency metric based on the amount of fuel required to move a given payload mass a certain distance. This new efficiency metric would be calculated as follows:

$$\eta = \frac{\sum(m_p \Delta X)}{\sum m_f} \tag{15}$$

Unfortunately, system-wide information on payload is not available at the level of resolution necessary to evaluate this metric. Aggregated load factors could be used as a possible surrogate for flight-by-flight payload estimates. The FAA reports aggregated monthly load-factor data provided by carriers. The load factors for the time frame we analyzed are provided in Table 7.

In the RSVM analysis, we did not analyze entire months, but instead selected weeks within each month. The information required to disaggregate these monthly load factors into individual weeks was not available. Additionally, we purposely excluded weeks that would be greatly affected by holiday travel, as holiday weeks will influence the monthly average load-factor estimates. Although different load factors would have an impact on efficiency in the pre- or post-RVSM data periods, it would have relatively less impact on the change in efficiency as a result of RVSM. Therefore, a comprehensive assessment of load factors was excluded.

VIII. Conclusions

We estimate that the implementation of RVSM over the domestic U.S. led to a 1.8% (±0.5%) improvement in fuel burn efficiency and a 3.1% (±1.2%) improvement in NOx. These estimates are consistent with the benefits estimated in the prior EUROCONTROL and FAA studies. However, this study analyzed flights for a longer period of time (one month before and one month after RVSM implementation), and improved upon the modeling techniques used in the prior studies. Notably, if we were to have used the standard BADA methods as used in the previous studies, we would have estimated essentially no improvement in fuel efficiency between the pre- and post-RVSM periods analyzed.

BADA methods were designed to provide fleet-level performance estimates. We developed methods that can be used to improve upon BADA methods when estimating small changes in operating conditions (such as those due to RVSM). Both the aircraft-specific, CFDR-derived SFC model and the model that is generalized for application to all jet-powered aircraft may be valuable to other researchers. However, the most significant factor influencing our estimates relative to prior studies was the inclusion of meteorological data. Approximately 70% of the difference in estimated efficiency benefit (both fuel and NOx) relative to the original BADA method

Table 7 U.S. domestic monthly load factors

	Nov-04	Dec-04	Jan-05	Feb-05	Mar-05
Ton-km available	3.08×10^{10}	3.29×10^{10}	3.06×10^{10}	2.9×10^{10}	3.32×10^{10}
Ton-km used	1.66×10^{10}	1.85×10^{10}	1.66×10^{10}	1.61×10^{10}	2.01×10^{10}
Load factor	0.538	0.562	0.543	0.556	0.605

can be attributed to including meteorological data, 18% to including a new SFC calculation, and 12% to measuring efficiency based on a metric of air distance traveled.

References

[1] Penner, J. E., Lister, D., Griggs, D. J., Dokken, D. J., McFarland, M., *Aviation and the Global Atmosphere*, Cambridge Univ. Press, Cambridge, England, U.K., 1999.

[2] "Reduced Vertical Separation Minimum," Federal Aviation Administration Air Traffic Organization, http://www.faa.gov/about/office_org/headquarters_offices/ato/service_units/enroute/rvsm/ [retrieved 2 Jan. 2008].

[3] Jelinek, F., Carlier, S., Smith, J, Quesne, A., "The EUR RVSM Implementation Project Environmental Benefit Analysis," EUROCONTROL, Rept. EEC/ENV/2002/008, Oct. 2002.

[4] "Benefit Analysis and Report for Domestic Reduced Vertical Separation Minimum (DRVSM)," Federal Aviation Administration Air Traffic Organization System Operations Services, Sept. 2005.

[5] "Enhanced Traffic Management System (ETMS), Functional Description, Version 7.6," U.S. Department of Transportation: Research and Innovative Technology Administration, Rept. VNTSC-DTS56-TMS-002, Aug. 2003.

[6] "*User Manual for the Base of Aircraft Data (BADA), Revision 3.6*," EUROCONTROL Experimental Center, Brussels, Sept. 2004.

[7] Lee, J. J., Waitz, I. A., Kim, B. Y., Fleming, G. G., Maurice, L., Holsclaw, C. A., "System for Assessing Aviation's Global Emissions (SAGE), Part 2: Uncertainty Assessment," *Transportation Research. Part D, Transportation and Environment*, Vol. 12, No. 6, Aug. 2007, pp. 381–395.

[8] Yoder, T., "Development of Aircraft Fuel Burn Modeling Techniques with Applications to Global Emissions Modeling and Assessment of the Benefits of Reduced Vertical Separation Minimums," Master's Thesis, Massachusetts Institute of Technology, May 2007.

[9] "Global Modeling and Assimilation Office," NASA Goddard Space Flight Center http://gmao.gsfc.nasa.gov/index.php [retrieved 2 Oct. 2006].

[10] Hill, P. G., and Peterson, C. R., *Mechanics and Thermodynamics of Propulsion*," 2nd ed., Addison Wesley Longman, Reading, MA, 1992.

[11] "ICAO Engine Exhaust Emissions Databank," International Civil Aviation Organization (ICAO), http://www.caa.co.uk/default. aspx?categoryid=702&pagetype=90 [retrieved 6 June 2005].

[12] DuBois, D. P., Paynter, G. C., "Fuel Flow Method 2 for Estimating Aircraft Emissions," Society of Automotive Engineers Paper 2006-01-1987, 2006.